Proceedings of the Iowa Academy of Science

Volume 73 | Annual Issue Article 34

1966

Void Ratio and Shear Strength of Two Compacted Crushed Stones

Fernando H. Tinoco
Iowa State University

Richard L. Handy
Iowa State University

James M. Hoover
Iowa State University

Void Ratio and Shear Strength of Two Compacted Crushed Stones[1]

FERNANDO H. TINOCO, RICHARD L. HANDY AND JAMES M. HOOVER[2]

Abstract: Triaxial compression tests of two crushed limestones of differing highway service records indicate a fundamental difference in their shear strength—void ratio relationship. Analyses were based on stress parameters at minimum sample volume, i.e., before there was significant sample dilation due to shear. The better service record sample compacted to higher density, and had a high effective angle of internal friction and zero effective cohesion. The other sample compacted to lower density and had a lower friction angle, but gained significant stability from effective cohesion. Repeated loading-unloading cycles reduced the cohesion, apparently due to modification of the sample structure.

Extrapolations of the results to zero void ratio agree with sliding friction data reported on calcite, or with triaxial parameters reported on carbonate rocks.

INTRODUCTION

Compacted crushed limestone has been in common use for many years as a base course for flexible pavements. In recent years the greatly increased traffic loads and intensities have resulted in mixed service records of this material. The present study is part of a larger research program being conducted at Iowa State to discover and compare strength characteristics of several Iowa crushed stones with varying service records, and if possible explain the performance differences and relate to compositional differences such as gradation or mineralogy.

BASIS OF THIS INVESTIGATION

The usual use of the Mohr stress circle in soils is to represent stress conditions at failure, with failure defined as the condition of the soil at the maximum deviator stress or maximum principal stress ratio. The Mohr failure envelope is the line representing the locus of points showing stress conditions on the failure plane. But since a Mohr circle also represents any two-dimensional stress condition of equilibrium, it can be used at any strain value before failure is reached. Thus the envelope formed by points of tangency to Mohr circles representing effective stresses for a given condition of the sample can be used to find the cohesion and angle of internal friction at that given condition.

In this study the selected condition is the minimum void ratio reached during the shear test. This condition was chosen because

[1] A report of Project HR-99 sponsored by the Iowa Highway Research Board with funds from the Iowa State Highway Commission and the Bureau of Public Roads. Project 516-S of the Engineering Research Institute, Iowa State University. Soil Research Lab. Contribution No. 66-6.

[2] Graduate Research Assistant, Professor and Assistant Professor of Civil Engineering, respectively, Iowa State University, Ames, Iowa.

it represents a time of maximum density, when stability and strength are presumed to be maximum. That is, although the Mohr stress parameters usually become larger as the test continues to failure, they then include energy used to increase the soil volume as grains move over one another to allow formation of continuous shear planes. When this happens, the soil structure is changed, and successive repetitions of loading were not expected to follow the same stress paths.

Another alternative might be to use the constant-volume condition, after the test has progressed to the point where the shear zone is at the critical void ratio. This condition also was rejected, since it would be very undesirable in a pavement.

At the minimum void ratio point, the rate of volume change within the sample is zero and no corrections are necessary due to this effect.

Materials and Testing Procedures

Two crushed stones were selected as representative of Iowa State Highway Commission approved crushed stone for rolled-stone bases. One is a weathered, moderately hard limestone of the Pennsylvania system. (Anderson and Welp, 1959) obtained from near Bedford, in Taylor County, Iowa; hereafter this will be referred to as the Bedford sample. The second is a hard dolomite of the Devonian system (Anderson and Welp, *loc. cit.*) obtained from near Garner, Hancock County, Iowa, and hereafter referred to as the Garner sample. Of the two, the Garner has the better service record.

X-ray diffraction analyses of powdered representative samples showed calcite as the predominant mineral in both stones, but there was a considerable difference in calcite-dolomite ratio 1:25 in the Bedford stone and one:1.16 in the Garner (Handy, 1965). X-ray tests on HCl-insoluble residues showed no montmorillonite in either sample, a small amount of 14 Å mineral (vermiculite or chlorite) in the Garner, a predominance of illite in both, plus kaolinite and quartz. Kaolinite in the Bedford stone was poorly crystalline. The percent of insoluble residues was 10.9% in the Bedford and 6.7% in the Garner. pH's and cation exchange capacities of the whole samples were closely comparable.

Engineering properties of the two crushed stones are shown in Table 1. The Bedford stone contains more gravel, less sand and more clay size particles, and has a measurable plasticity. The optimum moisture content for compaction is higher and the compacted density lower than for the Garner sample. The latter of course influences the void ratio, defined as the volume of voids divided by the volume of solids.

Four-inch diameter by 8-inch high specimens were prepared

Table 1. Representative Engineering Properties of the Two Crushed Stones.

	Bedford	Garner
Textural Composition		
Gravel (> 2.00 mm)	73.2%	61.6%
Sand (2.00-0.074 mm)	12.9	26.0
Silt (0.74-0.005 mm)	8.4	10.2
Clay (<0.005 mm)	5.5	2.2
Colloids (<0.001 mm)	1.7	1.4
Atterberg Limits, (<042 mm mat'l):		
Liquid Limit	20%	Non-
Plastic Limit	18%	plastic
Plasticity Index	2	
Standard AASHO-ASTM Density		
Optimum moisture content,	10.9%	7.6%
% dry soil weight	127.4 pcf	140.5 pcf
Dry density		
Specific Gravity (minus No. 10 *sieve fraction)*	2.73	2.88
AASHO Classification	A-1-b	A-1-a
Unified Classification	GW	GW

for triaxial testing by compacting the crushed stones to standard Proctor density in a vibratory mold.

The type of triaxial test used was the consolidated undrained test, in which the compacted, encased specimen is placed in the triaxial cell, the cell pressure is applied, and full consolidation is allowed to take place before testing. The drainage valve is then closed, and the axial load is applied at a constant strain rate of 0.01 in/min.

Similar procedures were employed to prepare and test the specimens compacted at modified Proctor density. These data are from the work of Best (1966).

The triaxial shear tests were run with continuous volume change and pore water pressure measurements. Data were reduced and plotted with the aid of computer programs.

Analysis of the Data

The results may be plotted as shown in Fig. 1, where void ratios are plotted versus the logarithms of σ_{3c} $\frac{(\sigma_1' - \sigma_3')}{2}$, and $\frac{(\sigma_1' + \sigma_3')}{2}$. Meanings of these terms are given in Appendix A.

This form of presentation was originated during the Cooperative Triaxial Shear Research Program of the Corps of Engineers described by Rutledge (1947), and later used by Henkel (1959 and 1960) for tests on both normal and overconsolidated clays.

The consolidation history of the sample is taken into consideration in triaxial testing by means of the following equations, after Bishop and Henkel (1957).

$$\frac{\sigma_1' - \sigma_3}{2\,\sigma e'} = \frac{\cos \varphi'_r}{1 - \sin \varphi'_r} \bullet \frac{c'_r}{\sigma_e'} + \frac{1 - \sin \varphi'_r}{\sin \varphi'_r} \bullet \frac{\sigma_e'}{\sigma_3'} \quad (1)$$

$$\frac{\sigma_1' - \sigma_3'}{2\,\sigma_e'} = C_1 + \tan\,\beta_1 \frac{\sigma_3'}{\sigma_e'} \qquad (2)$$

where

$$C_1 = \frac{1 - \sin\,\varphi'_r}{\cos\,\varphi'_r} \times \frac{c'_r}{\sigma_e'}, \quad \tan\,\beta_1 = \frac{1 - \sin\,\varphi'_r}{\sin\,\varphi'_r} \text{ and}$$

σ_e' is the equivalent consolidation pressure. The equivalent consolidation pressure corresponding to a void ratio e is defined as the pressure σ_e' for a point on the virgin branch of the consolidation diagram with the ordinate e.

Eq. (1) may be transformed into:

$$\frac{\sigma_1' - \sigma_3'}{2\,\sigma_e'} = C_2 + \frac{\sigma_1' + \sigma_3'}{2\,\sigma_e'} \bullet \tan\,\beta_2 \qquad (3)$$

where $c_r' = \dfrac{C_2\sigma_e'}{\cos\,\varphi_r'}$, and $\tan\,B_2 = \sin\,\varphi_r'$. Equation (3) is used in this paper to determine c_r' and φ_r'.

The parameters c_r' and φ_r' are termed, respectively, the "effective cohesion" and "effective friction" components of the shear strength, after Hvorslev (1937, 1960). The effective cohesion component is a function of the effective consolidation pressure σ_e', and therefore is a function of the void ratio. The effective angle of internal friction or effective friction component is a function of the effective normal stress, and is theoretically independent of the void ratio.

The components of shear strength defined in the foregoing paragraphs are primarily mathematical expressions of the results of shear tests, and may be called phenomenological components which have not yet been identified with specific intrinsic forces (Hvorslev, 1960).

The experimental determination of c_r' and φ_r' for saturated clays requires that samples fail at the same moisture content (or void ratio), but at different effective stresses to allow trangential fitting of an envelope to the different Mohr circles. This restriction does not allow the direct determination of c_r' and φ_r' in the laboratory. However, shear tests on normal and over-consolidated samples permit the calculation of these parameters by means of equations (1) or (3).

We may postulate that if the shear strength of a soil is indeed a function of its void ratio or water content, the line representing the locus of points of maximum shear stress versus void ratio or moisture content must be parallel to the line representing the virgin branch and/or the reloading or unloading branch of consolidation for the given soil. If this requirement is fulfilled for the soil being tested, then the shear strength is a unique function of the void ratio and effective stresses (Hvorslev).

Discussion

The data corresponding to the Bedford material are shown in figures 1, 2, 3, and 4. In addition to the usual consolidated-undrained tests, Bedford samples compacted at standard Proctor density were tested under consolidated-repeated shear conditions. The repeated shear test was performed in the following manner: the normal load was applied at the constant axial strain rate to a maximum axial deflection of 0.075 inches, after which the axial strain was reversed and run at the same rate back to zero deflection. This process was repeated two times. The third loading was carried to failure and/or to constant sample volume.

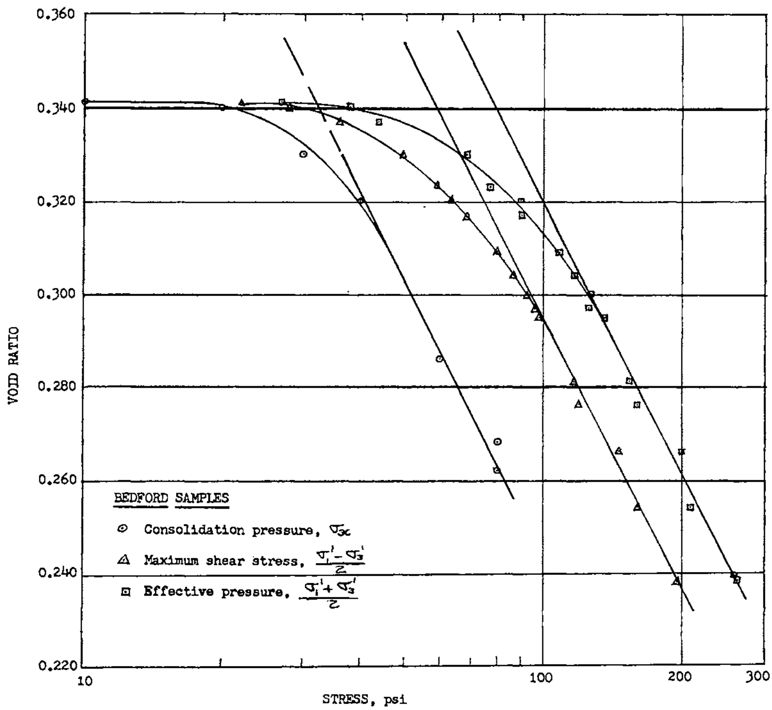

Figure 1. Bedford stone: consolidation pressure, maximum shear stress, and effective normal pressure as related to void ratio.

Figures 1 and 2 indicate that the shear strength of the Bedford crushed stone is a function of the void ratio, since as stated in the previous section, the shear stress-void ratio function is parallel to the consolidation pressure-void ratio function. Therefore, the caculation of the parameters c_r' and φ_r' is possible by a least

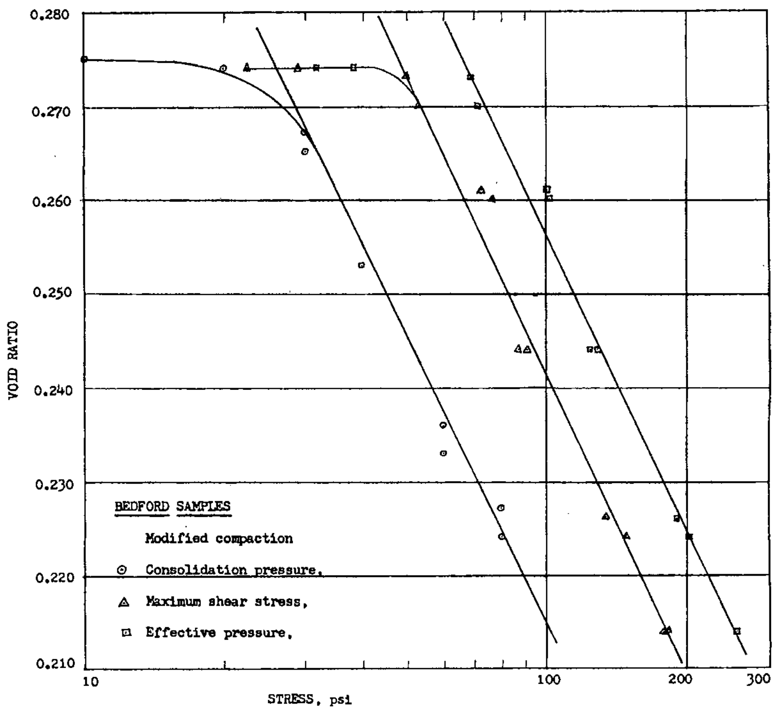

Figure 2. Bedford stone. consolidation pressure, maximum shear stress, and effective normal pressure as related to void ratio.

squares fit of equation (3), as shown in figure 3. Values obtained for these parameters are summarized in Table 2.

Table 2. Effective components of the shear strength of the Bedford stone.

Degree of Compaction	*Test Procedures*	c_r'	φ'
Standard Proctor	Normal	$1.160\sigma_e'$	45.6°
Standard Proctor	Repeated load	$0.027\sigma_e'$	46.2°
Modified Proctor	Normal	$0.223\sigma_e'$	41.0°

The parameter φ_r' for standard compaction differed very little in the two test procedures, and the difference can be attributed to errors involved in testing and other approximations. For the purpose of discussion, the parameter φ_r' is assumed to be the same for both testing procedures. Therefore, the strength difference between the two testing procedures is reflcted in the values of the parameter c_r'

Figure 4 shows the relationship between the logarithm of c_r' and the minimum void ratio of the sample during shear for the Bedford crushed stone. The repeated loading process reduced

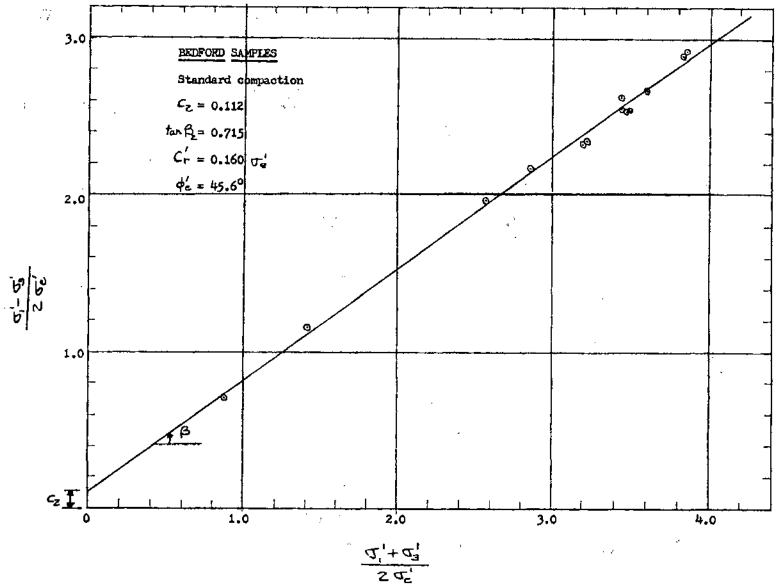

Figure 3. Bedford stone: relationship between $\frac{\sigma_1' - \sigma_3}{2\sigma_e}$ and $\frac{\sigma_1' + \sigma_3}{2\sigma_e}$.

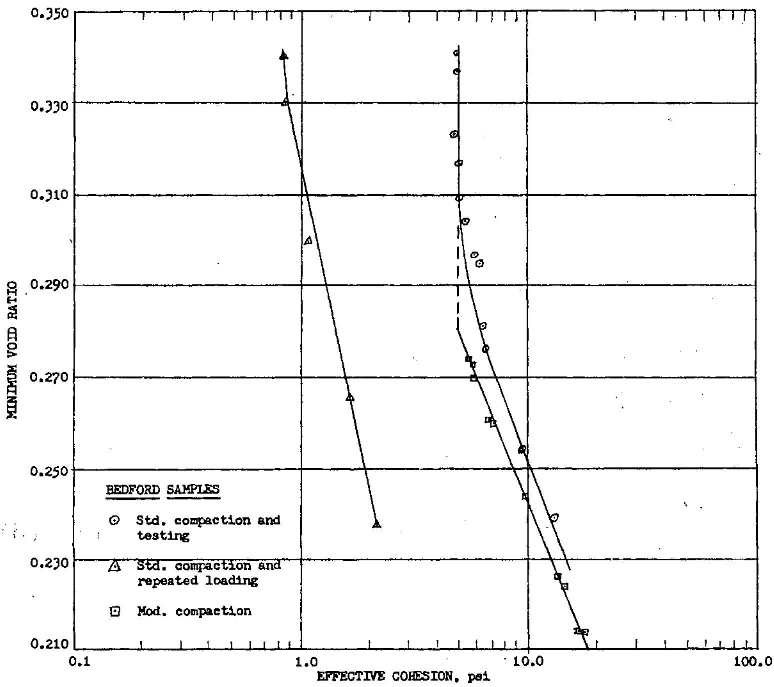

Figure 4. Bedford stone: relationship between the minimum void ratio and the effective cohesion.

the effective cohesion in each sample by 80% in comparison with the effective cohesion of the samples tested by the usual procedure. This reduction suggests a gradual change in the structure of the sample caused by the repeated loading process, and one may estimate that one more repetition might have reduced the sample to zero cohesion. It is observed in the same figure that this reduced cohesion value occurs in the same range of void ratios as the higher cohesion values of the samples tested by the usual method. Therefore the reduction in effective cohesion must in fact be due to a change in the structure rather than difference in void ratio. "Structure" is understood to mean the arrangement of soil particles and the electrical forces acting between adjacent particles (Lambe, 1958).

The gradual change from a "cohesive structure" to a "cohesionless structure" seems to depend on the amount of shearing strain imposed on the sample rather than on the stress level. It is noteworthy to indicate that the stress-strain curves were modified by the repeated loading process. However, the significance of such a change in the stress-strain diagram is outside the scope of this paper.

Figure 4 also shows that the effective cohesion of the standard compacted and tested Bedford sample is constant through the higher range of void ratio, whereas at lower values the effective cohesion becomes a linear function of the void ratio. The samples compacted at modified Proctor density also show a parallel linear relationship. Apparently a certain minimum compactness is required to achieve increasing cohesive strength with increasing density. The gradual change from a constant cohesion to a linearly increasing value with a decrease in void ratio probably indicates a change in structure.

Data corresponding to the Garner material are shown in figures 5, 6, and 7. Figures 5 and 6 indicate that $\frac{\sigma_1' - \sigma_3'}{2}$ and $\frac{\sigma_1' - \sigma_3'}{2}$ again are linear functions of the void ratio; they are expressed by:

$$\frac{\sigma_1' + \sigma_3'}{2} = 913 - 4075\, e_{min}, \qquad \text{for } e_{min} > 0.175 \qquad (4)$$

$$\frac{\sigma_1' - \sigma'_3}{2} = 662.5 - 2640\, e_{min}, \qquad \text{for } e_{min} < 0.175 \qquad (5)$$

$$\text{and } \frac{\sigma_1' - \sigma'_3}{2} = 1129 - 5030\, e_{min}. \qquad (6)$$

The effective cohesion, c_r', is zero for the Garner specimens. Therefore the friction component must be a function of the void ratio.

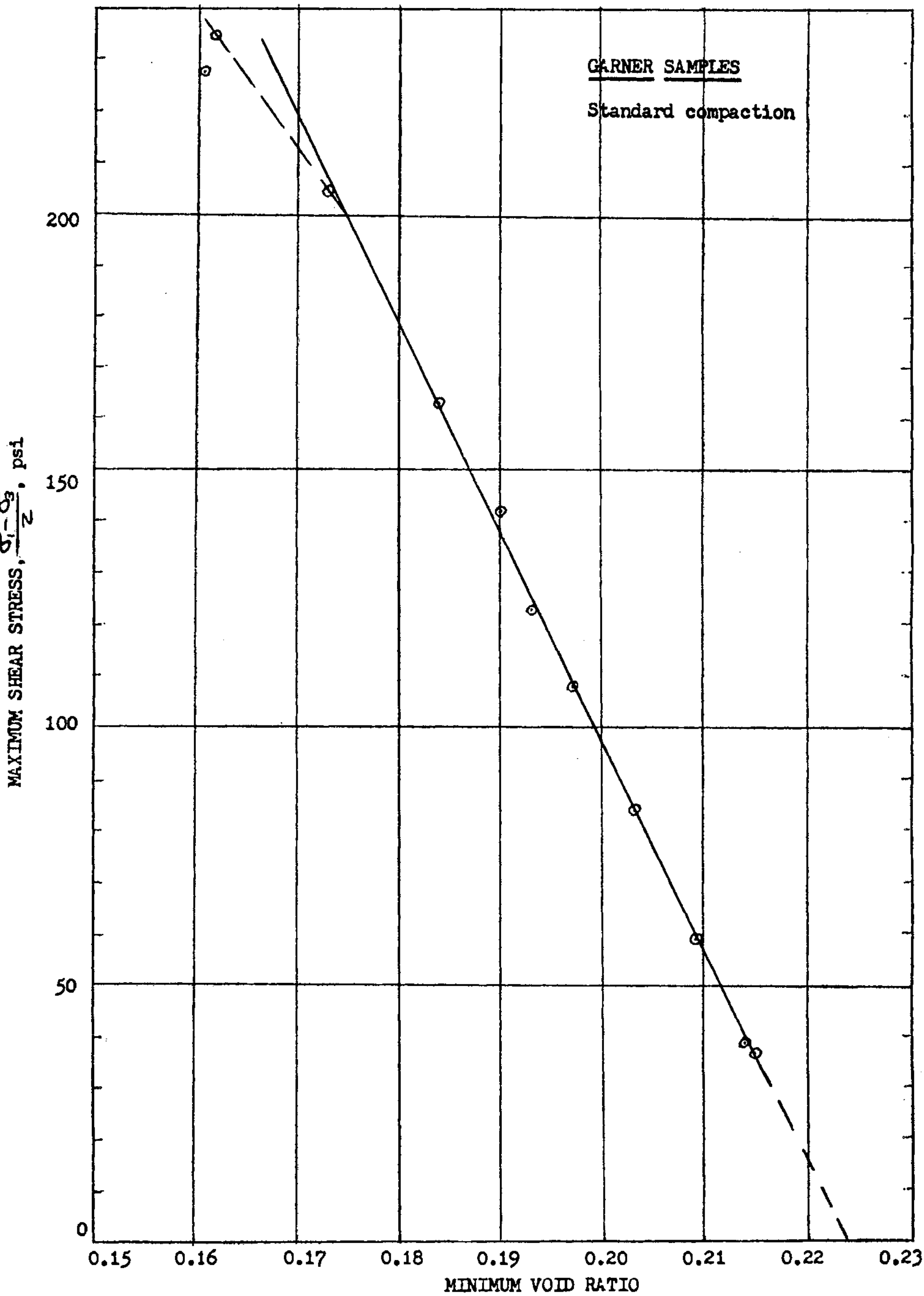

Figure 5. Garner Stone: maximum shear stress as related to minimum void ratio.

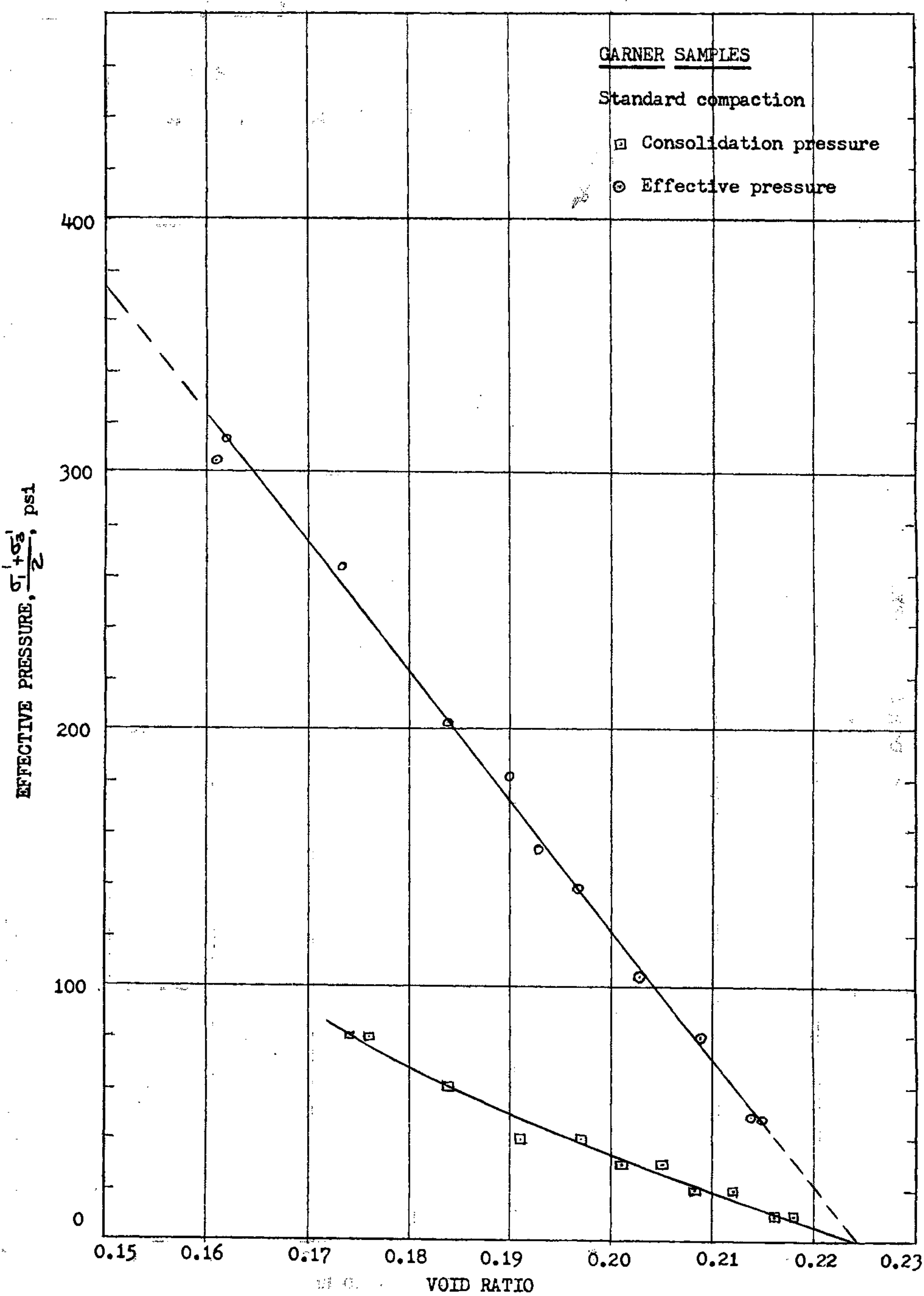

Figure 6. Garner stone: effective pressure and consolidation pressure as related to void ratio.

Figure 7 shows the relationship between sin φ' and the minimum void ratio, where sin φ' is given by the following equation:

$$\frac{\sigma_1' - \sigma_3'}{2} = \frac{\sigma_1' + \sigma_3'}{2} \sin \varphi' \tag{7}$$

Figure 7 indicates that the angle of friction, φ', increased as the void ratio decreased to a value 0.175. Once this void ratio was reached, there was a change in the relationship and sin φ' decreased as the void ratio decreased. This change may be due to increased effective pressure causing crushing of interparticle contacts, reducing friction between the particles. The beneficial increase of sin φ' with decrease in void ratio and increase in effective pressure may relate to an increasing number of interparticle contacts.

An interesting result is obtained when e_{min} is extrapolated to zero in equations (5) and (6):

$$\frac{\sigma_1' - \sigma_3'}{2} = 662.4 \ \& \ \frac{\sigma_1' + \sigma_3'}{2} = 1129, \text{ which gives sin}$$

$\varphi' = 0.587$ and $\varphi' = 35.9°$.

The predominant mineral in the Garner crushed stone is calcite. Horn (1961) found the friction between surfaces of pure calcite submerged in water was 34.3°, by using a slider which applies shear force on three small "feet" sticking out of the highly polished contact surfaces. The purpose was to obtain an area of contact as small as possible.

A similar extrapolation can be made for the Bedford crushed stone, as shown in Table 3.

Table 3. Shear strength components of the Bedford crushed stone calculated at $e_{min} = 0$.

Degree of Compaction	*Cohesion, psi*	*Angle of Friction, deg.*
Standard Proctor	1171	36.5
Modified Proctor	1116	39.9

Calcite is also the predominant mineral of the Bedford crushed stone. Von Karman (1911) performed triaxial tests on marble at very high cell pressure, up to 36,000 psi, and Bridgman (1936) and Griggs (1942) performed high pressure tests on calcite. The envelopes obtained are slightly curved and the mean results are summarized in Table 4, which also shows the results obtained for the Bedford material on the assumption that the friction angle was 34.0°, in order that a comparison could be drawn with the above quoted authors' results.

The implication of the above comparisons is that the behavior of the Bedford and Garner stones belongs in two different systems; the Garner extrapolates to pure sliding friction, whereas

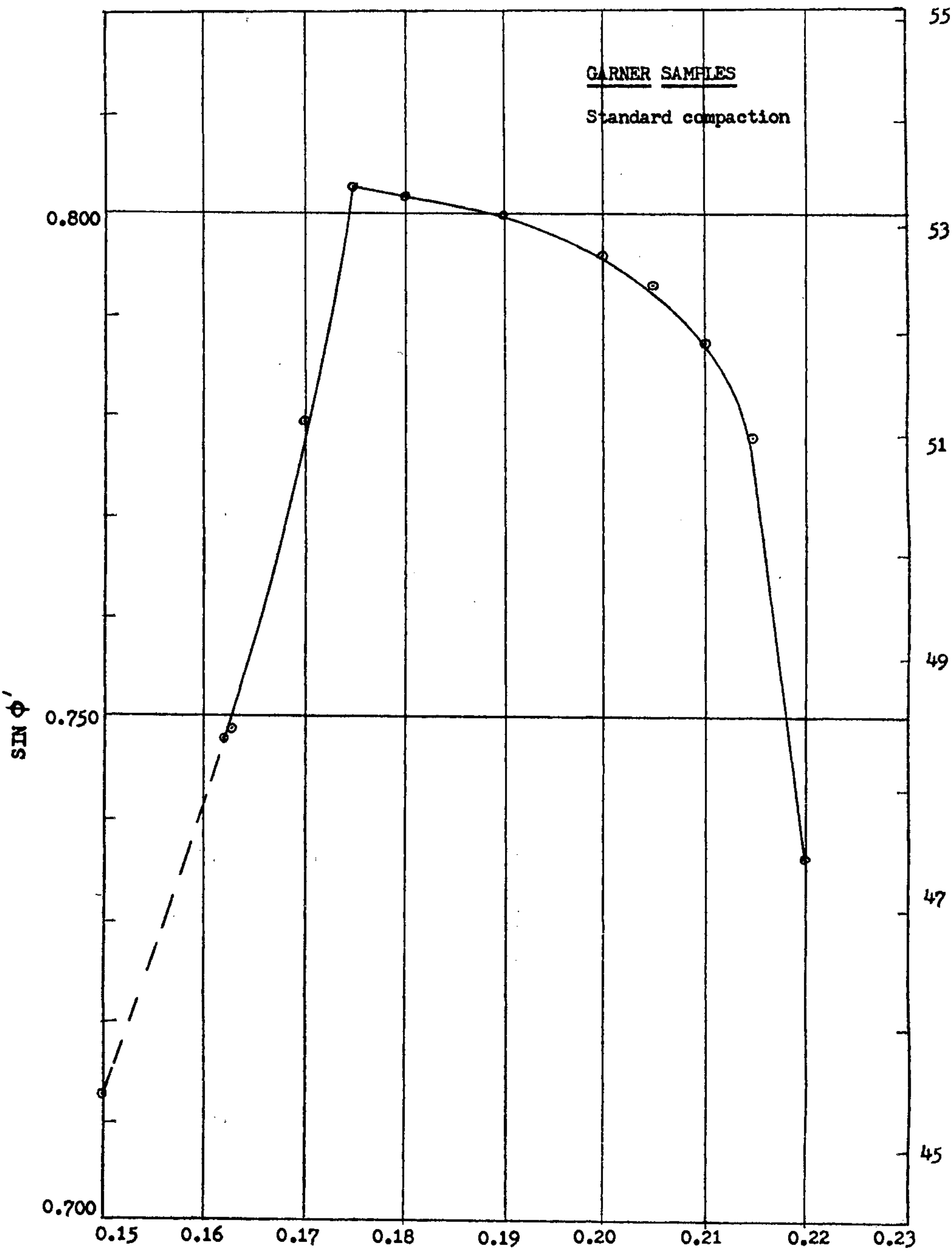

Figure 7. Garner stone: values of sin φ' and φ' as related to minimum void ratio.

Table 4. Shear strength components of calcite for $\sigma' < 80{,}000$ psi.

Author	*Rock*	*Cohesion, psi.*	*Angle of Friction, deg.*
Von Karman	Marble	4980	34
Bridgman & Griggs	Calcite	2990	34
Tinoco, et. al.	Bedford (Std. Comp.)	1315	34
Tinoco, et. al.	Bedford (Mod. Comp.)	3868	34

the Bedford extrapolates to sliding friction plus a cohesion comparable to values found in solid rock.

The exponential shear stress-void ratio function for the Bedford would appear to indicate increased cohesion caused by increased grain contact areas under higher pressures. This implies a compressibility of the Bedford stone particles. Under repeated loading, slight intergranular shear movements could perhaps cause the loss in cohesion, since grains would no longer be properly arranged or interlocked to cause an increase in contact areas with loading. That is, repeated compressions result in densification and a mass action rather than a point-contact building-block action of individual grains.

In the case of the Garner material, the shear stress-void ratio function is linear and therefore reflects the state of packing within the granular system. The friction parameter is therefore a measure of the interparticle interaction rather than the frictional characteristics of the particles. Thus most crushed stones, unlike the Bedford, tend to maintain strength under repeated loading.

Conclusions

The shear-stress-void ratio function is an index to the behavior of compacted crushed stone materials under shear. Two different types of behavior are inferred: (a) compression of particle contacts under loading, increasing cohesion and giving an exponential relationship between shear strength and void ratio, and (b) sliding at point contacts between particles, giving a linear relationship between shear strength and void ratio.

Behavior (a) apparently is not stable under repeated loading, since shear strength is gradually lost. This suggests a structural rearrangement of the grains which reduces grain-to-grain contact under pressure, and therefore cohesion. That is, the beneficial effect of consolidating pressures is gradually lost. Thus under repeated loading the behavior is similar to that of a clay.

In contrast, behavior (b) should be stable under repeated loading.

The difference in behavior of the two stones thus may relate to the compression and shear character of the individual grain-to-grain surface contacts, which in turn should relate to some petrographic characteristics of the rock.

Acknowledgements

The research reported herein is a portion of a project on "Factors Influencing Stability of Granular Base Course Mixes" under contract with the Iowa Highway Research Board, Iowa State Highway Commission and Bureau of Public Roads, U.S. Department of Commerce.

Sincere appreciation is extended to the following organizations and personnel: to the Iowa Highway Research Board and Bureau of Public Roads for their continuing support of this project; to Mr. Steve Roberts, Director of Research, Mr. Tom McElherne, Materials Engineer, and Mr. Ted Welp, Geologist, Iowa State Highway Commission, for their valuable assistance and counseling; and to Dr. Turgut Demirel, Iowa State University, for his advice, interest, and criticisms.

Literature Cited

Anderson, A. A. and Welp, T. L. 1960). "*An engineering report on the soils, geology, terrain and climate of Iowa.*" Iowa State Highway Commission. Ames, Iowa pp. 3-12.

Best, T. (1966). Private communication. Ames, Iowa.

Bishop, A. W. and Henkel, D. J. (1957). "*The measurement of soil properties in the triaxial test.*" 190 pages. Edward Arnold Ltd, London.

Bridgman, P. W. (1936). "Shearing phenomena at high pressures." Proc. Amer. Acad. Arts. Sci., 71, pp. 387-469. In Skempton, A. W. (1960). *Proc. of Conference on Pore Pressure and Suction in Soils.* Butterworths, London, pp. 4-16.

Handy, R. L. (1965). "Quantitative X-ray diffraction measurements by fast scanning." *Analytical Techniques for Hydraulic Cements and Concrete,* ASTM STP 395, Am. Soc. Testing Matl's., pp. 30-44.

Henkel, D. J. (1959). Geotechnique, Vol. 9, pp. 119-135.

——— (1960). Goetechnique, Vol. 10, pp. 41-54.

Horn, H. M. (1961). "An investigation of the frictional characteristics of minerals." Ph.D. Thesis. Department of Civil Engineering, University of Illinois, Urbana.

Hvorslev, M. J. (1937). "Ueber die Festigkeit seigenschaften gestörter bindiger Böden". Ingeniorvidenskabelige Skrifter A. No. 45, 159 pages. Reviewed in Hvorslev, M. J. (1960). "Physical components of the shear strength of saturated clays." *Research conference on Shear Strength of Cohesive Soils.* Am. Soc. Civ. Engr. Boulder, Colorado, pp. 169-273.

———, (1960). "Physical components of the shear strength of saturated clays." *Research Conference on Shear Strength of Cohesive Soils.* Am. Soc. Civ. Engr. Boulder, Colorado, pp. 169-273.

Griggs, D. T. (1942). Handbook of Physical Constants, Geol. Soc. America. Special Paper, No. 36, pp. 107-130. In Skempton, A. W. (1960). *Proc. of Conference on Pore Pressure and Suction in Soils.* Butterworths, London, pp. 4-16.

Karman, Th. Von (1911). "Festigkeitsversuche unter allseitigen Druck". *Ziet. Vereines Deutsch. Ing.,* 55, pp. 1749-57. In Skempton, A. W. (1960). Proc. of Conference on Pore Pressure and Suction in Soils. Butterworths, London, pp. 4-16.

Lambe, T. W. (1958). "The structure of compacted clay". *Proc. Am. Soc. Civ. Engr.* SMF Div., Vol. 84, No. SM2, Paper No. 1654.

Rutledge, P. C. (1947). "Review of cooperative triaxial research program of the Corps of Engineers". *Progress Report on Soil Mechanics Fact Finding Survey.* Waterways Experiment Station, Vicksburg, Mississippi, pp. 1-178.

APPENDIX A

Symbols used in this paper

σ'_{c3}	Effective consolidation pressure; i.e., applied consolidation pressure less pore pressure.
σ_1	Effective major principal stress.
$\frac{\sigma_1' - \sigma_3'}{2}$	Maximum shear stress
$\frac{\sigma_1' - \sigma_3'}{2}$	Effective mean pressure or effective pressure
σ_e'	Equivalent consolidation pressure which gives void ratio e under conditions of normal consolidation
c_r'	Effective cohesion
φ_r'	Effective angle of internal friction
c_1	Intercept of failure line for $\frac{\sigma_e'}{\sigma_3'} = 0$
c_2	Intercept of failure line for $\frac{\sigma_1' + \sigma_3'}{2\sigma'_e} = 0$
β_1	Angle that the failure line makes with horizontal axis, $\frac{\sigma_3'}{\sigma_e'}$
β_2	Angle that the failure line makes with horizontal axis, $\frac{\sigma_1' + \sigma_3'}{2\sigma_e}$